Thermochemistry of the activation of N_2 on iron cluster cations: Guided ion beam studies of the reactions of Fe_n^+ (n=1–19) with N_2

Lin Tan, Fuyi Liu, and P. B. Armentrout[a)]
Department of Chemistry, University of Utah, Salt Lake City, Utah 84112

(Received 28 November 2005; accepted 12 January 2006; published online 22 February 2006)

The kinetic energy dependences of the reactions of Fe_n^+ (n=1–19) with N_2 are studied in a guided ion beam tandem mass spectrometer over the energy range of 0–15 eV. In addition to collision-induced dissociation forming Fe_m^+ ions, which dominate the product spectra, a variety of $Fe_mN_2^+$ and Fe_mN^+ product ions, where $m \leq n$, is observed. All processes are observed to exhibit thresholds. Fe_m^+–N and Fe_m^+–2N bond energies as a function of cluster size are derived from the threshold analysis of the kinetic energy dependences of the endothermic reactions. The trends in this thermochemistry are compared to the isoelectronic $D_0(Fe_n^+–CH)$, and to bulk phase values. A fairly uniform barrier of 0.48±0.03 eV at 0 K is observed for formation of the $Fe_nN_2^+$ product ions (n=12, 15–19) and can be related to the rate-limiting step in the Haber process for catalytic ammonia production. © *2006 American Institute of Physics*. [DOI: 10.1063/1.2172240]

INTRODUCTION

The reaction of iron with dinitrogen is of considerable practical importance as dissociative chemisorption of dinitrogen is thought to be the rate-limiting step in the Haber process for the catalytic synthesis of ammonia from N_2 and H_2.[1,2] The industrial catalyst is Fe_3O_4 to which small amounts (1%) of Al_2O_3 and K_2O and sometimes other oxides are added as promoters.[3] A number of studies have examined the reaction of N_2 with iron surfaces, as reviewed elsewhere.[4] Previous work on the interaction of N_2 with Fe(100), (110), and (111) surfaces indicates that the dissociative chemisorption proceeds slowly with activation energies measured as ranging from nearly 0 (111) to 0.3 eV (110).[5–7] The reverse process, desorption of N_2 from iron surfaces, has been measured to have activation energies between 2.2 and 2.5 eV (depending on surface orientation). Combining this information yields an estimate for the strength of the Fe(s)–N bond as about 6.0 eV for the (100), (110), and (111) surfaces.[5,6] However, Stoltze and Nørskov have reanalyzed these data taking into account the low sticking coefficient of N_2 and obtain a much lower desorption energy of 1.67 eV, which yields a Fe(s)–N bond energy of 5.7 eV.[8] Additional work on the Fe(111) surface has indicated that the dissociative adsorption of N_2 occurs via a weakly bonded molecular precursor that has both N atoms interacting with the surface.[9,10] More recently, the adsorption of gases N_2, H_2, O_2, and NH_3 that play a role in ammonia synthesis have been studied on crystalline Fe surfaces by sum frequency generation (SFG) vibrational spectroscopy using an integrated ultrahigh vacuum/high-pressure system.[11] The diffusion of individual N atoms on Fe surfaces has been studied using scanning tunneling microscopy and density functional theory (DFT) calculations.[12]

Investigating the chemistry of transition metal clusters is currently an active frontier in chemical physics. One of the motivations for these studies is the idea that the clusters may serve as models for surfaces and heterogeneous catalysts. Studies of metal clusters of different charges and sizes have found that the reactivity can vary appreciably at small sizes, but that the size effects gradually vanish with increasing size.[13–23] For example, previous work in our laboratory finds that average gas-phase cluster bond energies extrapolate nicely to the bulk phase heat of vaporization as the cluster size increases.[24] Unfortunately, very little experimental information is available on the detailed electronic and geometric structures of transition metal clusters except for the smallest clusters.[13] Experimentally, the guided ion beam technique has proven to be successful in providing kinetic energy-dependent reaction cross sections, which can be interpreted to yield accurate bond energies for metal-ligand complexes[25] and ligated metal clusters.[26–38] Using this technology, our group has studied collision-induced dissociation (CID) of bare transition metal clusters[39–45] and their reactions with D_2, O_2, CO_2, ND_3, and CD_4,[27,28,33,46,47] in an ongoing effort to understand the reactivity, electronic structures, and geometry of transition metal clusters. These experimental studies have shown interesting variations with cluster size in the stability and reactivity of clusters.

In previous work, we examined the reactions of size-specific iron cluster cations with ammonia.[46] Among the products formed at high energies were the Fe_nN^+ ions. Thresholds for formation of these products were analyzed and bond energies for iron cluster cations bound to N were determined. The values obtained ranged from 3.6–4.9 eV for n=2–10 and 14. These bond energies seem low relative to values for Fe_n^+–CH, an isoelectronic species with bond energies ranging from 5.0 to 6.4 eV for n=3–15,[47] as well as the estimates for nitrogen atoms bound to bulk phase iron, which lie near 5.7–6.0 eV (see discussion above).[5,6,8,48] In an effort to redetermine these cluster nitride bond energies, the present work examines the reactions of size-specific iron cluster cat-

a)Electronic mail: armentrout@chem.utah.edu

ions with N_2 using guided ion beam tandem mass spectrometry. Despite the very strong N_2 bond energy of 9.76 eV,[49] activation of dinitrogen on such clusters is observed. The kinetic energy dependences of these reactions from near zero energies to approximately 15 eV are interpreted to yield thermodynamic information about both Fe_mN^+ and $Fe_mN_2^+$ as a function of the cluster size. Bond energies for the cluster nitride and dinitride cations are reported and compared to the previous values for Fe_m^+–N, Fe_m^+–CH, and bulk phase chemistry. A key to this analysis is the availability of quantitative thermochemistry regarding the stability of the bare iron clusters, previously measured in our laboratory.[39]

EXPERIMENTAL SECTION

The reactions of iron cluster cations with N_2 are studied using a guided ion beam tandem mass spectrometer equipped with a laser ablation cluster source. The experimental apparatus and techniques used in this work have been described in detail elsewhere.[50] The output of an Oxford ACL-35 copper vapor laser operating at 7–8 kHz is tightly focused onto a rotating and translating iron rod inside an aluminum source block. The optimum pulse energy for iron cluster ion production ranges between 3 and 4 mJ/pulse. The plasma thus created is entrained in a continuous flow of helium at a flow rate between 5000–6000 SCCM (standard cubic centimeter per minute). The helium is passed through a liquid N_2 cooled molecular sieve trap to remove impurities. Frequent collisions and rapid mixing leads to the formation of thermalized clusters (300 K) as they travel down a 2 mm diameter 6.3 cm long condensation tube that immediately follows the target. An average ion undergoes approximately 10^5 collisions with He in this channel, a number that should be sufficient to equilibrate the ions to the temperature of the He carrier gas. This seeded helium flow then undergoes a mild supersonic expansion in a field-free region and is skimmed. Although direct measurements of the internal temperatures of the clusters are not possible, iron cluster ions thus created are believed to be fully thermalized to 300 K and maybe cooler, as indicated by previous studies.[39]

Positively charged ions are accelerated, focused, and injected into a 60° magnetic sector momentum analyzer where clusters of a particular size are mass selected for further study. After selection, size-specific cluster ions having intensities of $0.5–1.0\times10^6$ ions/s are focused into an octopole ion-beam guide[51] that passes through a collision cell where the neutral gas (N_2) is introduced. The octopole ion beam guide utilizes rf electric fields to create a potential well that traps ions in the transverse direction without affecting their axial energy. The pressure of N_2 neutral reactant gas in the reaction cell is kept relatively low to reduce the probability of multiple collisions with the ions. To test this, all studies were conducted at two pressures of N_2, ~0.2 and ~0.4 mTorr. Product and remaining cluster ions drift out of the collision chamber to the end of the octopole, where they are extracted and injected into a quadrupole mass filter for mass analysis. The quadrupole has a mass limit of ~1100 amu such that iron cluster reaction products up to $Fe_{19}N_2^+$ can be studied. Finally, ions are detected by a 27 kV conversion dynode, secondary electron scintillation ion counter,[52] and the signal is processed using standard counting techniques. Conversion of detected ion intensities into reaction cross sections is treated as discussed previously.[53] The experimental total reaction cross section, σ_{tot}, is determined by the relation $I_R=(I_R+\Sigma I_P)\exp(-\sigma_{tot}\rho l)$, where I_R and I_P are the measured transmitted intensities of the reactant and product ions, respectively, ρ is the gas density, and l is the effective path length. Individual product cross sections, σ_P, are found by the formula $\sigma_P=\sigma_{tot}(I_P/\Sigma I_P)$.[53] Absolute cross sections measured in our laboratory have an uncertainty estimated as ±30%, with relative uncertainties ±5%. The accuracy of these absolute reaction cross sections has been verified upon a number of occasions both by comparison with theoretical collision cross sections and with other experimental data.[53–55]

Results for each reaction system were repeated several times to ensure their reproducibility. CID experiments with Xe were performed on all the cluster ions to ensure their identity and the absence of any excessive internal excitation. In all instances, CID thresholds are consistent with those previously reported.[39] The absolute zero in the kinetic energy and the corresponding full width at half maximum (FWHM) of the ions were measured using the octopole as a retarding energy analyzer.[53] The error associated with the absolute energy scale is 0.05 eV in the laboratory frame with a FWHM varying from 0.5–2.2 eV (laboratory). Kinetic energies in the laboratory frame are converted to center-of-mass (CM) energies using the stationary target approximation, $E(\mathrm{CM})=E(\mathrm{laboratory})\ M(N_2)/[M(N_2)+M(Fe_n^+)]$ where $M(Fe_n^+)$ is the cluster ion mass and $M(N_2)$ is the mass of dinitrogen (28.00 amu).

Products observed in this work include $Fe_mN_2^+$, Fe_mN^+, and Fe_m^+. In order to efficiently collect all products throughout the wide energy range of interest, the resolution of the quadrupole mass filter is set fairly low, but this leads to overlap of adjacent mass peaks. Because the energy dependences of the various products are usually distinct, such overlap is easily identified and eliminated. The cross sections shown here have been corrected for such overlaps.

RESULTS

In all systems, the reactions were carried out from near zero energies to 15 eV in the center-of-mass frame. Fe_n^+ reactant clusters ranging in size from $n=1–19$ were studied. In all systems except for $n=1$, the dominant reactions observed are the CID processes, reaction (1), in which Fe atoms are lost sequentially.

$$Fe_n^+ + N_2 \rightarrow Fe_m^+ + (n-m)Fe + N_2. \quad (1)$$

At higher energies, two other products are also observed in reactions (2) and (3).

$$Fe_n^+ + N_2 \rightarrow Fe_mN_2^+ + (n-m)Fe \quad (2)$$

$$\rightarrow Fe_mN^+ + N + (n-m)Fe. \quad (3)$$

In reaction (3), it is also possible that an FeN molecule is formed, a possibility discussed further below. As a general

nomenclature, we will refer to $Fe_mN_2^+$ products as "cluster dinitrides," Fe_mN^+ products as "cluster nitrides," and Fe_m^+ products as "cluster fragments," where $m \leq n$ for reaction of Fe_n^+. N_2^+ and N^+ ions are not observed in the reactions of any iron cluster because the ionization energies of N_2 and N, 15.58 and 14.53 eV, respectively,[49] are much higher than those of any iron containing products. In the discussion that follows, results for the smaller clusters are examined in detail, followed by an overview of those for larger clusters.

It was verified that the magnitude of the cross sections measured for reactions (2) and (3) where $n-m=0$, i.e., those that do not lose iron atoms, do not depend on the N_2 pressure, indicating that these cross sections correspond to the reactions of a single collision between reactants. In contrast, cross sections for the products corresponding to loss of one or more iron atoms exhibit a pressure dependence, as do cross sections for the CID reactions (1), as discussed and analyzed in detail previously for collisions with Xe.[39] This sensitivity to pressure can be explained as follows. At any finite N_2 pressure, there is a small probability for an iron cluster ion to undergo two collisions with N_2 in the gas cell (and increasingly smaller probabilities for additional collisions). Because the center-of-mass collision energies are well above thermal, such extra collisions deposit additional energy into the cluster ion, which has two effects: it lowers the observed experimental threshold, and it shortens the cluster ion lifetime and thereby greatly enhances the probability of observing dissociation near the threshold for single collision events. This latter effect will be most prominent for large parent cluster ions because they have longer dissociation lifetimes. The means to remove these pressure dependent effects has been outlined in a previous study.[45] Briefly, we acquire the data at two N_2 pressures, a fairly high value of ~0.4 mTorr and a low value of ~0.2 mTorr, and extrapolate the product cross sections to zero N_2 pressure. This eliminates the effects of secondary collisions and yields cross sections that are the exclusive result of single collisions.[39] All analysis is performed on the pressure extrapolated data.

$Fe_n^+(n=1-3)+N_2$

Atomic Fe^+ ions react with N_2 in only a single endothermic process to form $FeN^+ + N$, Fig. 1. Because of the conditions used to generate these Fe^+ ions, they are believed to be largely in their ^6D ground state.[56] The cross section for this reaction rises from a threshold of ~7 eV and reaches a peak of about 0.5 $Å^2$ near 14 eV. The location of this peak cross section contrasts with the behavior of many other reactions between atomic ions and diatomic neutrals where the maximum cross section occurs near the bond energy of the reactant diatomic X_2. This behavior occurs because the channel for forming $Fe^+ + 2X$ opens at this energy and unless energy is carried away in translational degrees of freedom of the $FeX^+ + X$ products, dissociation of the FeX^+ product should begin near this energy. The behavior observed here for N_2, where $D_0(N_2)=9.76$ eV,[49] therefore indicates that the reaction deposits considerable energy into translation of the products, thereby moving the onset for product dissociation to much higher energies. This observation suggests that the threshold for reaction (3) might also be shifted above the thermodynamic limit.

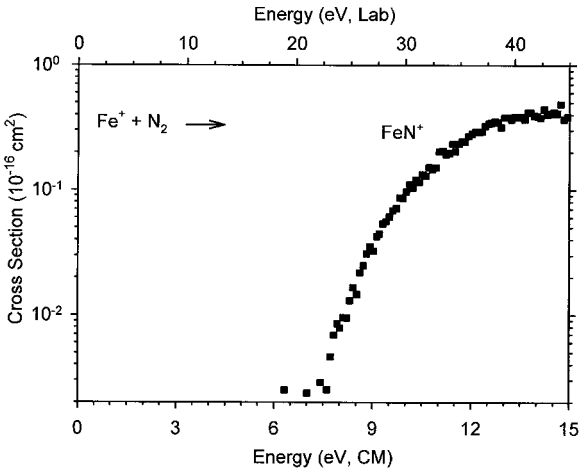

FIG. 1. Cross section for the reaction of Fe^+ with N_2 as a function of collision energy in the center-of-mass (lower x axis) and laboratory (upper x axis) frames.

The addition of a second iron atom to the reactant ion increases the complexity of the reaction, Fig. 2. Although there are only four atoms in the $Fe_2^+ + N_2$ system, there are five possible metal-containing ionic products, Fe^+, Fe_2N^+, FeN^+, $Fe_2N_2^+$, and FeN_2^+, but neither of the dinitrides are observed, as shown in Fig. 2. The dominant product over the most of the energy range examined is the Fe^+ fragment. This product rises from a threshold near 2 eV, which agrees with the previously measured behavior in collisions with Xe,[39] indicating that the simple CID reaction (1) is responsible for the formation of the Fe^+ product observed. The Fe_2N^+ cross section rises rapidly with energy beginning at ~7.5 eV, reaches a peak near 10 eV, and then declines, corresponding with an increase in the FeN^+ cross section. The sum of these two cross sections changes smoothly with energy, indicating that Fe_2N^+ is decomposing to $FeN^+ + Fe$, which suggests that the bond energy of Fe^+-N is larger than that of Fe^+-Fe, 2.74 eV.[39] Although this conclusion is not definitive in this

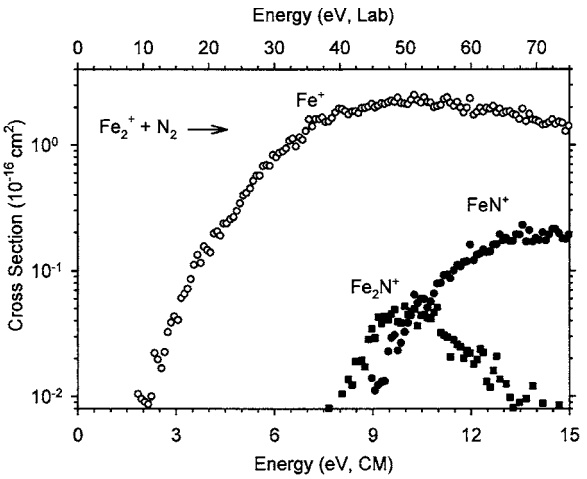

FIG. 2. Cross section for the reaction of Fe_2^+ with N_2 as a function of collision energy in the center-of-mass (lower x axis) and laboratory (upper x axis) frames.

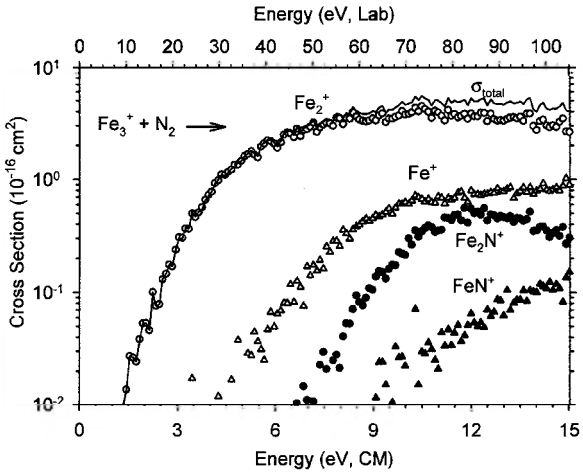

FIG. 3. Cross section for the reaction of Fe_3^+ with N_2 as a function of collision energy in the center-of-mass (lower x axis) and laboratory (upper x axis) frames.

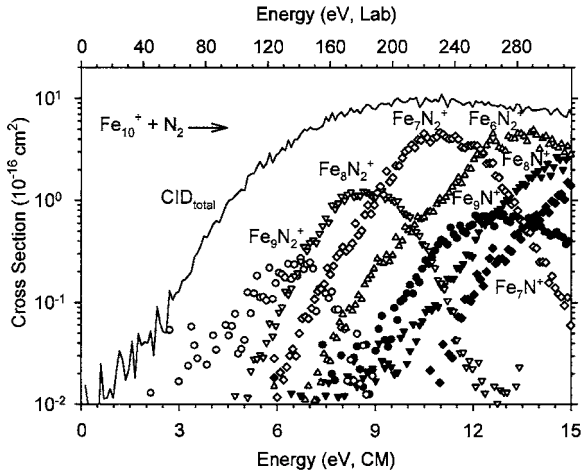

FIG. 5. Cross section for the reaction of Fe_{10}^+ with N_2 as a function of collision energy in the center-of-mass (lower x axis) and laboratory (upper x axis) frames.

case because dissociation of Fe_2N^+ to Fe_2^++N reforms the reactant ion and therefore cannot be explicitly monitored, the thermochemistry determined below confirms this qualitative result.

In the reaction of the iron trimer cation with N_2, there are seven possible metal-containing reaction products, four of which are observed, Fe_2^+, Fe^+, Fe_2N^+, and FeN^+, Fig. 3. We looked for the Fe_3N^+ product but did not observe it or any cluster dinitrides. The dominant product ion seen, Fe_2^+, results from simple CID as the apparent threshold of this channel is in agreement with $D_0(Fe_2^+-Fe)=1.67\pm0.12$ eV.[39] At higher energies, Fe^+ results from further decomposition with a threshold comparable to $D_0(Fe_2^+-Fe)+D_0(Fe^+-Fe)=4.41\pm0.12$ eV.[39] Observation of the Fe_2N^+ product could be accompanied by two possible neutral products, FeN or Fe+N. If the latter products were formed, then we might have expected to see either the Fe_3N^+ or $Fe_2N_2^+$ products, although it is possible that these ions have intensities that are too small to observe easily. These two possibilities are explored further below when the energetics of the reactions are analyzed, where it is confirmed that the neutral products are Fe+N. The FeN^+ ion is assigned to be a secondary product stemming from the decay of the primary Fe_2N^+ product. Its energetic behavior is consistent with that observed in the Fe_2^++N_2 system, although the relative intensities differ because formation of Fe_2N^+ is accompanied by two neutral atoms here, which leads to a colder internal energy distribution of the Fe_2N^+ ions formed here compared to those produced in the Fe_2^++N_2 system.

$Fe_n^+(n=4-19)+N_2$

Figures 4–6 show results for the reactions of Fe_4^+, Fe_{10}^+, and Fe_{19}^+ with N_2, respectively. Results for all remaining clusters are available in supporting information.[57] These three systems are representative of the behavior of all clusters larger than Fe_3^+. For all these larger clusters, product ions are dominated by formation of cluster fragment ions. For $n=2-19$ clusters, the thresholds for formation of these CID products are essentially equal to those measured in the Fe_n^++Xe system.[39] Magnitudes are also similar for small clusters,

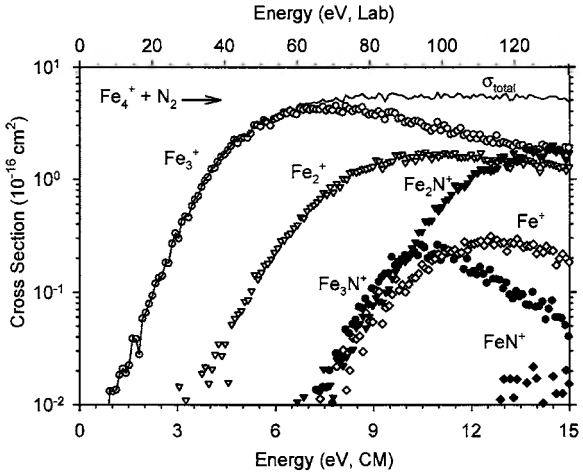

FIG. 4. Cross section for the reaction of Fe_4^+ with N_2 as a function of collision energy in the center-of-mass (lower x axis) and laboratory (upper x axis) frames.

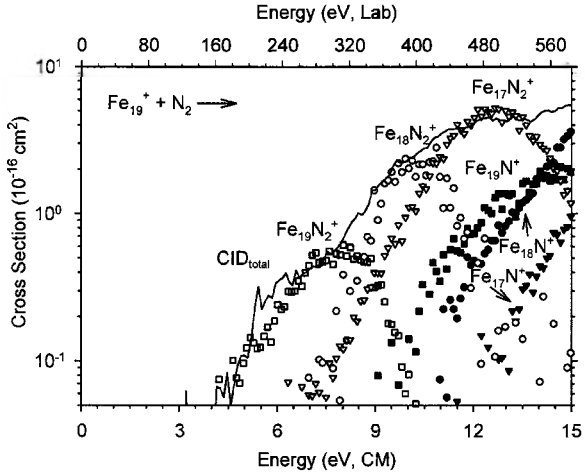

FIG. 6. Cross section for the reaction of Fe_{19}^+ with N_2 as a function of collision energy in the center-of-mass (lower x axis) and laboratory (upper x axis) frames.

but for larger clusters ($n=15-19$), the magnitudes are smaller than those obtained with Xe by a factor of ~2.

As for the reaction of the trimer, all larger iron cluster ions react to form cluster mononitride product ions in reaction (3) where $n-m=1$ and 2. For Fe_n^+ where $n \geq 15$, we also find the Fe_nN^+ product ion (i.e., $n-m=0$). The Fe_nN^+ and $Fe_{n-1}N^+$ product cross sections exhibit thresholds in the range of 7–10 eV, and then these products dissociate by sequentially losing iron atoms as the energy increases, Figs. 4–6. This is apparent from the observation that the Fe_mN^+ product cross section reaches a maximum as the $Fe_{m-1}N^+$ cross section reaches a comparable magnitude.

Cluster dinitride product ions begin to be observed at $n=6$, where the $Fe_4N_2^+$ ion is observed. All larger iron clusters also form the $Fe_{n-2}N_2^+$ product ion in reaction (2). From $n=9-19$, the $Fe_{n-1}N_2^+$ is also formed and is reasonably large. The $Fe_nN_2^+$ adduct is not observed until Fe_{12}^+. Although not observed for $n=13$ and 14, this species becomes fairly prominent at low energies for Fe_{16}^+ and larger clusters, Fig. 6. The cross sections for these cluster dinitride product ions are not dependent on the pressure of the N_2 reactant, so that collisional stabilization is not contributing to their formation. Apparently, as the size of the cluster increases, the lifetime of the product ion increases, thereby allowing the product to be observed. Thus, the smaller clusters need to lose two iron atoms to stabilize the $Fe_mN_2^+$ species ($m=n-2$) to the point where they can be observed on our experimental time scale of10^{-4} s. Larger clusters have sufficiently long lifetimes that $Fe_mN_2^+$ is observed after losing only one Fe atom ($m=n-1$), and eventually none ($m=n$). In all cases, the formation of the $Fe_nN_2^+$ adduct exhibits an appreciable threshold for formation, which demonstrates that it cannot be assigned to a simple physisorbed dinitrogen complex. Such a $Fe_n^+(N_2)$ complex should exhibit no barrier to its formation because of the attractive long-range ion-induced dipole potential between Fe_n^+ and N_2.

It is clear that the cluster dinitrides formed at low energies dissociate by sequential loss of iron atoms as the energy is increased. This behavior is evident from the observation that the cross sections for $Fe_mN_2^+$ products decline as the $Fe_{m-1}N_2^+$ cross sections rise to comparable magnitudes, Figs. 5 and 6. If there are any features that might correspond to formation of clusters of iron neutrals, they are negligible within our experimental signal to noise ratio. This behavior is another indication that the N–N bond is no longer intact in these molecules, as loss of N_2 would be expected at much lower energies than loss of iron atoms.

THRESHOLD ANALYSIS AND THERMOCHEMISTRY

Data analysis

The energy dependence of the cross sections for endothermic processes in the threshold region is modeled using Eq. (4),

$$\sigma(E) = \sigma_0 \Sigma g_i (E + E_i - E_0)^N / E, \tag{4a}$$

where σ_0 is an energy-independent scaling parameter, N is an adjustable parameter, E is the relative kinetic energy, and E_0 is the threshold for the reaction at 0 K. The summation is over the reactants' rovibrational states i having energies E_i and populations g_i, where $\Sigma g_i = 1$. We assume that the relative reactivity, as reflected by σ_0 and N, is the same for all rovibrational states. Details about our implementation of this equation are given elsewhere.[58–60] Briefly, the Beyer-Swinehart algorithm[61–63] is used to evaluate the density of the ion vibrational states, and then the relative populations, g_i, are calculated by the appropriate Maxwell-Boltzmann distribution at 300 K. Vibrational frequencies for the bare metal clusters are obtained by using an elastic model proposed by Shvartsburg *et al.*[64] The use of Eq. (4), which explicitly includes E_i, to analyze the threshold behavior of the cross sections makes the statistical assumption that the internal energy of the cluster is available to affect dissociation. This is appropriate because both the rotational and vibrational energies of the reactants are redistributed throughout the cluster upon impact with the collision gas. If the model truly measures the threshold (the least amount of energy necessary) for dissociation, then this threshold must correspond to the formation of products with no internal energy. Thus the thresholds obtained correspond to 0 K values.[65] Equation (4) has been used successfully in reproducing the cross sections of various ion-molecule reactions,[66–69] including CID and the reaction processes of transition metal cluster ions.[27–33,39–47] Before comparison with the data, this model cross section is also convoluted with the kinetic energy distribution of the ion and neutral reactants.[53]

For metal clusters, we account for the possibility that the processes being modeled occur more slowly than the experimental time window available, ~10^{-4} s in our apparatus. Because metal clusters have many low frequency vibrational modes, the lifetime of the transient intermediate can exceed the experimental time available for reaction. Thus, an important component of the modeling of these reactions is to include their lifetime, as estimated using statistical Rice-Ramsperger-Kassel-Marcus (RRKM) theory.[63,70,71] Thus, Eq. (4a) converts to

$$\sigma(E) = (N\sigma_0/E) \sum_i g_i \int_{E_0-E_i}^{E} [1 - e^{-k(E^*)\tau}](E-\varepsilon)^{N-1} d(\epsilon), \tag{4b}$$

where ε is the energy deposited in the complex by the collision, $E^* = \varepsilon + E_i$ is the internal energy of the energized molecule (EM), τ is the experimental time available for dissociation, $k(E^*)$ is the unimolecular rate constant as defined by RRKM theory, and all other parameters are the same as in Eq. (4a). The implementation of RRKM theory in the present work is detailed elsewhere[58] and requires the vibrational frequencies and rotational constants of the nitrogenated and bare clusters along with the reaction degeneracy. For all species, the $3n-6$ vibrations associated with the iron atoms are assumed to equal those of the bare cluster. Three additional frequencies are needed for each nitrogen atom and are taken from our study of the reactions of Fe_n^+ with ND_3.[46] For Fe_nN^+, we increase the frequency of the HFe_2-NH_2 stretch measured by Kauffman *et al.*[72] (581 cm^{-1}) to account for the increase in the bond order of Fe_n^+-N vs $Fe_n^+-NH_2$, which yields a frequency of 712 cm^{-1}. The two additional frequen-

cies for the wag and asymmetric stretch of Fe_nN^+ (655 and 541 cm^{-1}) are estimated from the ratio of these frequencies for Fe_nD^+.[27,33] For $Fe_nN_2^+$, we assume both nitrogen atoms bind to two chemically equivalent positions and use the same three vibrational frequencies for each N atom. For all cluster sizes, the cluster-ligand frequencies were assumed to remain constant. Although this is undoubtedly not precise, clusters differing by only one iron atom should have frequencies that do not differ appreciably. Rotational constants of the bare metal and the nitrogenated clusters were chosen using procedures outlined previously.[27]

For reactions leading to Fe_nN^+, reactions (3) with $n-m=0$, the EM is the transiently formed $Fe_nN_2^+$ complex, which we assume has a NFe_nN^+ structure, for reasons discussed above, and the reaction degeneracy is 2. For reactions leading to $Fe_mN_x^+$ ($m<n$, $x=1$ and 2), reactions (2) and (3), the EM is the transiently formed $Fe_{m+1}N_x^+$ complex, with reaction degeneracies of m for $x=1$ and $m-1$ for $x=2$, where iron atoms bound to N atoms are presumed not to dissociate. The choice of the transition state (TS) and its molecular constants is one of the more challenging aspects of any unimolecular decomposition calculation. Because the products analyzed here are formed by the loss of several atoms, we believe that the most reasonable choice places the TS at the point where the last atom is lost from the nitrogenated cluster, Fe for all $Fe_mN_2^+$ and $Fe_mN^+(m<n)$ products and N for the Fe_nN^+ products. The data were analyzed assuming both a loose transition state (LTS) and a standard transition state (STS). In our LTS model, the transition state is located at the variationally determined centrifugal barrier of the ion-induced-dipole potential and has vibrational and rotational parameters equivalent to the two product fragments.[58] Because the loss of Fe or N from these clusters involves the cleavage of a strong covalent bond, it seems likely that this transition state is too loose.[73] The STS uses molecular parameters from the EM with one frequency removed as a reaction coordinate and with two adjacent vibrational frequencies reduced by a factor of 2 for the transitional modes. The STS model is the model used in our previous studies of metal cluster dissociation,[39–45,50,74] and therefore parallels the treatment previously used for the loss of metal atoms.

Including these factors, Eq. (4) can accurately model the experimental cross sections from threshold to high energies. The parameters of Eq. (4), σ_0, N, and E_0, are varied until the model reproduces the data optimally as determined by a nonlinear least squares method. Uncertainties in the listed E_0 values include errors associated with variations in E_0 over the range of N values that adequately reproduce several data sets, variations in the vibrational frequencies of the reactant cluster ions, energized molecules, and transition states by factors of 1/2 and 2, and the absolute uncertainty in the energy scale (0.05 eV, laboratory). Thus, the uncertainties include all known random and systematic uncertainties in the data acquisition and analysis.

Cluster dinitride bond energies, Fe_m^+-2N

The bond of N_2 ($D_0=9.76$ eV) is very strong,[49] such that formation of $Fe_mN_2^+$ dinitride products in endothermic reactions for all reactant cluster ions studied is not surprising. Therefore, measurements of the Fe_m^+-2N bond energies can be obtained by using Eq. (4) to analyze the energy dependence of the cross sections for formation of cluster dinitrides in these endothermic processes. For clusters larger than $n=9$, cross sections for the $Fe_{n-1}N_2^+$ products, called the primary products, were analyzed. For clusters larger than $n=6$, we analyzed the cross sections for the $Fe_{n-2}N_2^+$ products, which we call the secondary products, and for clusters $n=6-16$, the cross sections for the "tertiary" $Fe_{n-3}N_2^+$ products were also studied. Hence, we have up to three independent means of determining the thermochemistry for the $Fe_mN_2^+$ products. The optimized parameters used in Eq. (4) to reproduce the data are listed in Table I and converted to $Fe_mN_2^+$ thermochemistry for the primary ($x=1$), secondary ($x=2$), and tertiary ($x=3$) products by using Eq. (5),

$$D_0(Fe_m^+-2N)=D_0(Fe_{n-x}^+-xFe)+D_0(N_2)-E_0(m=n-x), \quad (5)$$

where the sequential bond energies of the bare metal cluster ions, $D_0(Fe_{n-x}^+-xFe)$, are taken from our previous CID studies.[39] The 0 K bond energies derived from these threshold determinations are listed in Table II to allow the comparison between values from different systems. The uncertainties in the secondary and tertiary values are relatively large because of the combined uncertainties of the $D_0(Fe_{n-1}^+-Fe)$, $D_0(Fe_{n-2}^+-Fe)$, and $D_0(Fe_{n-3}^+-Fe)$ values.

Results for the LTS and STS models yield very similar bond energies for the smallest clusters because the kinetic shifts are small, whereas for larger clusters, the tighter STS leads to a larger kinetic shift, lower thresholds, and thus larger bond energies (by up to about 0.8 eV) for all reaction pathways. Patterns in the bond energies as a function of cluster size are the same for both the LTS and STS models. For the STS model results, Fig. 7 shows that the Fe_m^+-2N bond energies derived from the primary $Fe_{n-1}N_2^+$ product thresholds agree reasonably well with the energies from the secondary $Fe_{n-2}N_2^+$ and tertiary $Fe_{n-3}N_2^+$ product thresholds for all clusters studied. Similar agreement is obtained among the LTS model results. Average deviations between the primary and secondary values ($m=8-17$) are 0.33 (LTS) and 0.37 (STS) eV, between the primary and tertiary values ($m=8-13$) are 0.13 (LTS) and 0.39 (STS) eV, and between the secondary and tertiary values ($m=4-13$) are 0.23 (LTS) and 0.16 (STS) eV. These differences are within the combined uncertainties of the corresponding values. The average bond energies of these various independent values (up to three) are taken as our best values, Table II.

For clusters $n=12$ and 15–19, cross sections for the $Fe_nN_2^+$ products, called direct products, were also analyzed. In the case of $n=12$, it appears that the particularly strong Fe_{12}^+-2N bond energy, Fig. 7 and Table II, probably contributes to allowing the observation of this product. For the largest clusters studied, direct product cross sections may be observed because of the increases in the lifetime of the dissociating cluster relative to our experimental time scale. Note that for Fe_{12}^+, the thermochemistry of Table II indicates that formation of $Fe_{12}N_2^+$ is exothermic (by 1.02 ± 0.55 eV),

TABLE I. Summary of parameters of Eq. (4) for analysis of the cross sections for reactions $Fe_n^+ + N_2 \rightarrow Fe_mN_2^+ + (n-m)Fe$. (Uncertainties of one standard deviation are in parentheses. LTS=loose transition state. STS=standard transition state).

n	m	σ_0	N	E_0. eV (LTS)	E_0. eV (STS)
6	4	0.47(0.11)	1.1(0.2)	5.41(0.16)	5.42(0.16)
	3	0.18(0.04)	1.2(0.2)	8.26(0.14)	8.33(0.13)
7	5	3.51(1.00)	1.2(0.3)	5.73(0.19)	5.66(0.14)
	4	16.7(3.4)	1.1(0.2)	8.74(0.13)	8.74(0.11)
8	6	4.48(1.21)	1.2(0.3)	5.57(0.18)	5.42(0.12)
	5	4.29(1.53)	1.3(0.3)	8.31(0.20)	8.15(0.15)
9	8	0.45(0.13)	1.2(0.4)	3.44(0.14)	3.18(0.12)
	7	3.69(0.99)	1.1(0.3)	5.94(0.13)	5.62(0.11)
	6	11.0(3.1)	1.2(0.3)	8.51(0.16)	8.14(0.12)
10	9	0.55(0.13)	1.2(0.2)	3.11(0.11)	2.90(0.10)
	8	5.42(1.48)	1.2(0.3)	5.93(0.12)	5.53(0.10)
	7	25.9(6.8)	1.2(0.3)	8.96(0.12)	8.48(0.11)
11	10	1.16(0.39)	1.2(0.3)	3.16(0.16)	2.95(0.13)
	9	8.48(2.73)	1.1(0.3)	6.10(0.15)	5.68(0.12)
	8	22.1(6.0)	1.2(0.3)	9.18(0.12)	8.65(0.10)
12	12	1.45E6(0.93E6)	1.7(0.3)		0.50(0.04)[a]
	11	1.29(0.66)	1.2(0.4)	2.98(0.29)	2.85(0.21)
	10	15.1(2.6)	1.1(0.3)	6.28(0.08)	5.85(0.07)
	9	21.0(7.2)	1.2(0.3)	9.59(0.16)	9.01(0.13)
13	12	1.50(0.50)	1.1(0.3)	3.33(0.16)	3.10(0.13)
	11	10.9(2.5)	1.1(0.2)	6.83(0.09)	6.30(0.07)
	10	28.0(6.9)	1.2(0.3)	10.58(0.09)	9.88(0.08)
14	13	0.79(0.35)	1.2(0.3)	2.66(0.35)	2.60(0.27)
	12	13.8(2.8)	1.0(0.3)	6.52(0.08)	5.98(0.07)
	11	30.4(8.2)	1.1(0.3)	9.73(0.11)	9.02(0.09)
15	15	1.47E6(1.18E6)	1.7(0.3)		0.46(0.05)[a]
	14	0.67(0.38)	1.2(0.3)	3.08(0.34)	2.94(0.24)
	13	11.4(3.0)	1.2(0.3)	6.42(0.10)	5.96(0.08)
	12	3.50(1.06)	1.2(0.3)	9.88(0.12)	9.05(0.10)
16	16	1.34E6(0.83E6)	1.9(0.5)		0.49(0.03)[a]
	15	1.57(0.61)	1.3(0.3)	3.38(0.16)	3.14(0.13)
	14	6.82(1.81)	1.1(0.3)	6.83(0.10)	6.25(0.08)
	13	1.97(0.54)	1.2(0.3)	9.59(0.10)	8.74(0.08)
17	17	6.18E6(4.44E6)	1.7(0.4)		0.52(0.01)[a]
	16	6.81(3.02)	1.1(0.3)	3.98(0.15)	3.65(0.12)
	15	32.1(12.4)	1.1(0.4)	7.08(0.12)	6.72(0.10)
18	18	1.53E7(0.57E7)	1.5(0.3)		0.45(0.02)[a]
	17	5.33(2.27)	1.2(0.3)	3.57(0.15)	3.26(0.12)
	16	63.2(17.0)	1.3(0.3)	6.83(0.08)	6.26(0.05)
19	19	4.80E7(2.05E7)	1.5(0.4)		0.46(0.04)[a]
	18	12.7(4.9)	1.2(0.2)	4.05(0.10)	3.62(0.08)
	17	31.9(9.6)	1.2(0.3)	7.31(0.10)	6.63(0.08)

[a]A tight transition state is assumed. see text.

whereas the reaction is essentially thermoneutral for $n=15-18$. The observation that these direct reactions exhibit appreciable barriers, see Fig. 6, suggests that their thresholds do not correspond to the thermodynamic limit for $Fe_nN_2^+$ formation, but rather are equivalent to the activation energies for chemisorption of N_2 on iron clusters. Likewise, for clusters $n=4-6$ and 10–14, the cluster dinitride bond energies we measure (Fig. 7 and Table II) are greater than the bond energy of N_2 (9.76 eV), such that formation of the $Fe_nN_2^+$ direct dinitride products for these clusters is exothermic. Presumably this reaction is not observed in these cases (except for $n=12$) because these small clusters rapidly dissociate by losing Fe atoms once the barrier for formation of $Fe_nN_2^+$ is surmounted.

To model these direct reactions, we assume that the energized molecule is $Fe_n(N_2)^+$ in which an N_2 molecule is physisorbed to an iron cluster. This species can either activate the N_2 molecule, yielding the long-lived $Fe_nN_2^+$ dinitride products observed, or can dissociate by losing N_2. Because dissociation is much more likely than activation, this explains why the apparent thresholds for the direct products are shifted to relatively high energies. We model the direct product cross sections by assuming two competitive channels: (a) the product channel back to $Fe_n^+ + N_2$ reactants, which has a loose transition state and no reverse activation barrier, and (b) formation of the cluster dinitrides over an activation barrier described as a tight transition state (TTS). In this model, the molecular parameters of the TTS are assumed to equal

TABLE II. Summary of 0 K bond energies (in eV) for Fe_m^+–2N from data in Table I. (Uncertainties of one standard deviation are in parentheses. LTS =loose transition state. STS=standard transition state).

	Primary[a]		Secondary[b]		Tertiary[c]		Average[d]	
m	LTS	STS	LTS	STS	LTS	STS	LTS	STS
3					9.20 (0.42)	9.13 (0.42)	9.20 (0.42)	9.13 (0.42)
4			9.93 (0.38)	9.93 (0.38)	9.72 (0.45)	9.72 (0.45)	9.83 (0.34)	9.83 (0.34)
5			10.20 (0.41)	10.27 (0.39)	10.02 (0.50)	10.18 (0.48)	10.11 (0.38)	10.23 (0.36)
6			9.70 (0.42)	9.85 (0.40)	9.45 (0.53)	9.83 (0.52)	9.58 (0.40)	9.84 (0.39)
7			8.92 (0.45)	9.24 (0.44)	8.64 (0.55)	9.12 (0.55)	8.78 (0.41)	9.18 (0.41)
8	9.02 (0.36)	9.28 (0.35)	9.27 (0.48)	9.67 (0.48)	9.00 (0.60)	9.53 (0.59)	9.10 (0.40)	9.49 (0.39)
9	9.39 (0.35)	9.60 (0.34)	9.38 (0.50)	9.80 (0.50)	9.14 (0.65)	9.72 (0.64)	9.30 (0.46)	9.71 (0.42)
10	9.59 (0.39)	9.80 (0.37)	9.71 (0.54)	10.14 (0.54)	9.43 (0.72)	10.13 (0.71)	9.57 (0.47)	10.02 (0.46)
11	10.03 (0.50)	10.16 (0.45)	10.22 (0.62)	10.73 (0.62)	10.01 (0.78)	10.72 (0.78)	10.08 (0.52)	10.54 (0.52)
12	10.45 (0.49)	10.68 (0.49)	9.97 (0.67)	10.51 (0.67)	10.31 (0.82)	11.14 (0.81)	10.24 (0.55)	10.78 (0.55)
13	9.81 (0.58)	9.87 (0.54)	9.75 (0.66)	10.21 (0.66)	9.68 (0.83)	10.53 (0.83)	9.74 (0.56)	10.20 (0.56)
14	10.38 (0.57)	10.52 (0.52)	9.73 (0.69)	10.31 (0.68)			10.05 (0.52)	10.42 (0.50)
15	9.48 (0.52)	9.72 (0.52)	8.92 (0.72)	9.28 (0.71)			9.20 (0.53)	9.50 (0.52)
16	8.92 (0.52)	9.25 (0.52)	9.09 (0.73)	9.66 (0.72)			9.01 (0.53)	9.45 (0.52)
17	9.21 (0.54)	9.52 (0.53)	9.13 (0.62)	9.81 (0.62)			9.17 (0.49)	9.66 (0.47)
18	9.37 (0.33)	9.80 (0.33)					9.37 (0.33)	9.80 (0.33)

[a]From results for $Fe_n^+ + N_2 \rightarrow Fe_{n-1}N_2^+ + Fe$.
[b]From results for $Fe_n^+ + N_2 \rightarrow Fe_{n-2}N_2^+ + 2Fe$.
[c]From results for $Fe_n^+ + N_2 \rightarrow Fe_{n-3}N_2^+ + 3Fe$.
[d]Weighted average (one standard deviation) of available primary, secondary, and tertiary values.

those of the $Fe_n(N_2)^+$ complex (the EM) minus the single mode that corresponds to the reaction coordinate.[58] Analysis of the cross sections yields very consistent thresholds for all the direct products (n=12, 15–18), with an average value of E_0=0.48±0.03 eV. This value can be favorably compared with the previous work that estimates that the activation barrier for dinitrogen dissociation on Fe surfaces is greater than 0.35–0.43 eV.[48] Although Boszo *et al.* have measured activation energies of 0–0.3 eV,[5,6] Benziger has suggested that the very low reactivity of dinitrogen on iron surfaces may mean that these measured barriers actually correspond to diffusion away from surface defect sites where the activation actually occurs.[48]

Cluster nitride bond energies, Fe_m^+–N

As a first approximation to the cluster nitride bond energies, we can assume that the two nitrogen bonds in the $Fe_mN_2^+$ species are similar, i.e., that $D_0(Fe_m^+-N)$ is approximately half the $D_0(Fe_m^+-2N)$ values listed in Table II. This estimate gives Fe_m^+–N bond dissociation energies smaller than $D_0(N_2)$ for all clusters, indicating that reactions (3) must be endothermic in all cases, in agreement with our observations, Figs. 1–6. Formation of the cluster nitride product ions must clearly involve N_2 activation and the loss of a nitrogen atom from a dinitride complex, and thus reactions (3) are in direct competition with reaction (2). The experimental results clearly indicate that loss of an iron atom in reaction (2) is the more favorable process for larger clusters, indicating that the cluster-nitrogen bonds are stronger than the cluster-iron bonds. This is also shown by the observation that as the energy increases, the initially formed Fe_nN^+ product ion decomposes by sequential loss of iron atoms, not by N atom loss.

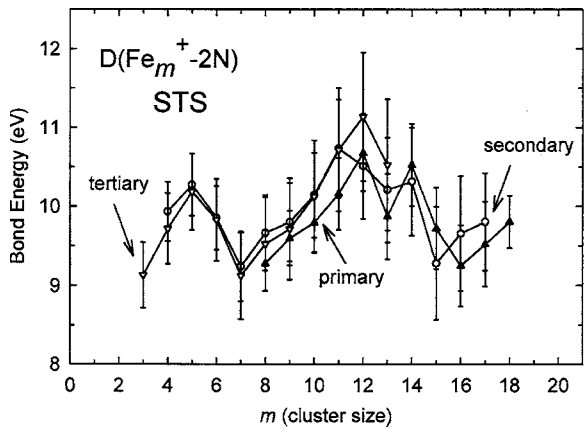

FIG. 7. Comparison of the 0 K cluster dinitride bond energies obtained from primary (closed triangles), secondary (open circles), and tertiary (open inverted triangles) measurements listed in Table II as a function of the number of iron atoms m.

For clusters larger than n=2, cross sections for the $Fe_{n-1}N^+$ product, called primary, were analyzed. For clusters larger than n=3, analysis included cross sections for the secondary $Fe_{n-2}N^+$ products. For clusters n=1, 2, and 15–19, cross sections for the direct Fe_nN^+ products were analyzed. Reactions (3) are analyzed using Eq. (4) with both LTS and STS models and the optimized parameters are given in Table III. The threshold energies for reactions (3) can be converted to Fe_m^+–N bond energies by using Eqs. (6) and (7),

$$D_0(Fe_m^+ - N) = D_0(N_2) - E_0(m = n), \tag{6}$$

$$D_0(Fe_m^+ - N) = D_0(Fe_{n-x}^+ - xFe) + D_0(N_2) - E_0(m = n - x), \tag{7}$$

where the bond energies of the bare iron cluster ions have been measured previously.[39] The resulting 0 K bond energies are listed in Table IV and shown in Fig. 8. Primary and secondary values agree reasonably well with average devia-

TABLE III. Summary of parameters of Eq. (4) for analysis of the cross sections for reactions $Fe_n^+ + N_2 \rightarrow Fe_mN^+ + (n-m)Fe + N$. (Uncertainties of one standard deviation are in parentheses. LTS=loose transition state. STS=standard transition state).

n	m	σ_0	N	E_0, eV (LTS)	E_0, eV (STS)
1	1	0.34(0.17)	1.7(0.3)	7.21(0.27)	7.21(0.27)
2	2	0.29(0.09)	1.0(0.3)	8.02(0.25)	8.02(0.25)
	1	0.46(0.08)	1.2(0.1)	9.38(0.12)	9.38(0.12)
3	2	1.17(0.42)	1.3(0.2)	7.08(0.24)	7.08(0.24)
	1	0.23(0.04)	1.2(0.1)	10.60(0.13)	10.60(0.13)
4	3	0.80(0.22)	1.2(0.2)	7.13(0.18)	7.13(0.18)
	2	3.90(1.41)	1.3(0.2)	8.45(0.25)	8.49(0.25)
5	4	0.46(0.13)	1.2(0.2)	7.87(0.19)	7.86(0.19)
	3	3.12(1.08)	1.3(0.2)	9.15(0.25)	9.15(0.25)
6	5	0.40(0.12)	1.3(0.3)	8.26(0.21)	8.16(0.17)
	4	4.24(1.40)	1.2(0.2)	10.40(0.15)	10.40(0.15)
7	6	3.77(0.82)	1.2(0.2)	8.82(0.12)	8.49(0.11)
	5	18.1(4.1)	1.3(0.1)	10.90(0.14)	10.92(0.14)
8	7	6.55(1.56)	1.3(0.2)	8.83(0.12)	8.44(0.11)
	6	30.0(8.5)	1.3(0.2)	11.11(0.19)	10.97(0.14)
9	8	2.62(0.75)	1.1(0.2)	8.82(0.14)	8.39(0.13)
	7	8.84(2.91)	1.4(0.2)	11.29(0.20)	10.90(0.15)
10	9	2.60(0.89)	1.3(0.2)	8.69(0.16)	8.24(0.14)
	8	21.2(4.5)	1.2(0.3)	11.97(0.10)	11.36(0.09)
11	10	2.90(0.79)	1.3(0.2)	8.92(0.12)	8.49(0.10)
	9	18.5(6.0)	1.1(0.3)	12.17(0.16)	11.51(0.14)
12	11	4.16(1.22)	1.2(0.2)	8.87(0.14)	8.33(0.12)
	10	12.1(5.1)	1.4(0.4)	12.37(0.18)	11.66(0.11)
13	12	6.10(2.01)	1.3(0.2)	9.34(0.17)	8.74(0.16)
	11	6.39(2.52)	1.3(0.4)	12.56(0.15)	11.77(0.13)
14	13	4.76(1.83)	1.3(0.2)	8.94(0.15)	8.44(0.13)
	12	13.6(3.5)	1.3(0.3)	12.36(0.14)	11.46(0.10)
15	15	2.73(1.07)	1.0(0.3)	5.93(0.12)	5.93(0.12)
	14	4.73(1.21)	1.3(0.2)	9.21(0.10)	8.54(0.07)
	13	8.83(2.85)	1.2(0.2)	12.16(0.06)	11.38(0.06)
16	16	3.59(1.30)	1.0(0.2)	5.71(0.10)	5.71(0.10)
	15	15.7(6.3)	1.4(0.2)	9.52(0.11)	8.85(0.09)
	14	6.47(1.28)	1.2(0.3)	12.67(0.07)	11.79(0.06)
17	17	4.05(1.26)	1.0(0.2)	5.70(0.09)	5.70(0.09)
	16	6.63(2.44)	1.5(0.2)	9.14(0.17)	8.52(0.14)
	15	7.32(1.54)	1.0(0.3)	12.44(0.08)	11.51(0.06)
18	18	2.41(1.14)	1.3(0.3)	4.81(0.18)	4.81(0.18)
	17	8.43(3.42)	1.3(0.3)	8.62(0.15)	7.92(0.12)
	16	2.15(0.57)	1.1(0.3)	11.54(0.09)	10.58(0.07)
19	19	6.84(3.18)	1.1(0.3)	5.31(0.12)	5.31(0.12)
	18	29.0(9.7)	1.3(0.3)	9.75(0.14)	8.94(0.12)
	17	14.6(4.5)	1.1(0.4)	12.53(0.10)	11.66(0.08)

tions of 0.22±0.39 (LTS) and 0.30±0.39 (STS) eV for $m=1-17$. For smaller clusters where the kinetic shifts are small, bond energies of Fe_m^+-N derived from the STS and LTS models are comparable, but as the clusters get larger, the STS values become systematically higher than the LTS values (by up to about 0.7 eV for primary products and 0.9 eV for secondary products). Both sets of values are in reasonable agreement with bond energies obtained from previous work where the nitrogen source was ammonia, Fig. 8.[46] Average deviations between literature values and those determined here range from about 0.3 to 0.5 eV, depending on the transition state assumptions used, with the STS approach giving better agreement (by about 0.1 eV) compared to the LTS approach and primary values agreeing slightly better (by about 0.04 eV) compared to the secondary results. The better agreement with the STS method is partly because the literature values are obtained by using a TTS for formation of Fe_nN^+ from $Fe_nND_2^+$ and $Fe_{n+1}ND_2^+$ precursors. The direct values for large clusters ($m=15-19$) also give bond energies in reasonable agreement with the other available values. In contrast, the 2.55 eV value obtained from the direct reaction, $Fe^+ + N_2 \rightarrow FeN^+ + N$, is well below the mononitride bond energy, $D_0(Fe^+-N)=3.35\pm0.15$ eV, obtained as the average bond energies from the $Fe_2^+ + N_2 \rightarrow FeN^+ + Fe + N$ and $Fe_3^+ + N_2 \rightarrow FeN^+ + 2Fe + N$ reactions. Similarly, the direct reaction gives a Fe_2^+-N bond energy well below those for the primary and secondary pathways, Fig. 8. As noted above, there is evidence that the direct reactions for $n=1$ and 2 deposit considerable energy into translation of the products, thereby moving the onset for product formation and dissociation to much higher energies. This is presumably because the smallest iron clusters cannot easily break the very strong N_2 triple bond. Although such dynamic arguments are sufficient to explain the behavior observed for these direct products, it is also possible that there are barriers along the potential energy surface in these reactions.

Although the agreement between the primary, secondary, direct, and literature bond energies for the cluster nitrides is reasonable, it is possible that the thresholds for all of these processes are shifted to higher values by competition with other product channels. In the present system, the competition comes primarily between reaction channels (2) and (3) which form $Fe_{n-1}N_2^+$ and Fe_nN^+ from the same energized molecule ($Fe_nN_2^+$). Because the Fe atom loss is a lower energy and more probable process, the N atom loss channel can be suppressed such that the apparent thresholds for formation of the cluster nitrides may be shifted to higher energies and thus the bond energies determined above will be lower limits to the true bond energies. This shift would propagate for the direct, primary, and secondary processes, such that the bond energies derived from them could be self-consistent.

Unfortunately, because the $Fe_{n-1}N_2^+$ and Fe_nN^+ products are observed for only a couple of the largest clusters, the competition cannot be determined directly in most cases. In order to estimate the effect of such competitive shifts for all clusters, we have used the following procedure. First, thresholds for formation of Fe_nN^+ are estimated using the average STS bond energies of the cluster dinitrides from Table II, as shown in Eq. (8)

$$E_0(Fe_nN^+) = D_0(N_2) - D_0(Fe_n^+ - N) = D_0(N_2) - D_0(Fe_n^+ - 2N)/2. \quad (8)$$

Using a statistical model for competition between parallel reaction channels[75] [an extension of the Eq. (4) modeling procedure outlined above] and an STS model, cross sections are then calculated for formation of $Fe_{n-1}N_2^+$ and Fe_nN^+ using parameters for N and σ_0 that reproduce the experimental cluster dinitride product ion (as well as Fe_nN^+ for the largest clusters), i.e., those in Table I. The synthesized Fe_nN^+ cross section is then modeled using the same procedure as described above for the cluster nitride product ions, using the

TABLE IV. Summary of 0 K bond energies (in eV) for Fe_m^+–N from data in Table III and the literature. (Uncertainties of one standard deviation are in parentheses. LTS=loose transition state. STS=standard transition state).

	Direct[a]	Primary[b]		Secondary[c]		Literature[d]	Average[e]	
m		LTS	STS	LTS	STS	TTS	LTS	STS
1	2.55 (0.22)	3.12 (0.16)	3.12 (0.16)	3.57 (0.20)	3.57 (0.20)		3.35 (0.15)[f]	3.35 (0.15)[f]
2	1.74 (0.25)	4.35 (0.27)	4.35 (0.27)	5.05 (0.34)	5.05 (0.34)	4.95 (0.33)	4.78 (0.25)[f]	4.78 (0.25)[f]
3		4.74 (0.27)	4.74 (0.27)	5.25 (0.39)	5.25 (0.39)	4.62 (0.13)	4.87 (0.26)	4.87 (0.26)
4		4.42 (0.30)	4.43 (0.30)	4.95 (0.37)	4.95 (0.37)	4.96 (0.13)	4.78 (0.26)	4.78 (0.26)
5		4.56 (0.33)	4.66 (0.30)	5.03 (0.39)	5.01 (0.39)	4.47 (0.22)	4.69 (0.26)	4.71 (0.26)
6		4.05 (0.30)	4.38 (0.29)	4.16 (0.43)	4.30 (0.41)	4.30 (0.19)	4.17 (0.28)	4.33 (0.26)
7		3.33 (0.30)	3.72 (0.29)	3.57 (0.47)	3.96 (0.45)	4.03 (0.30)	3.64 (0.29)	3.90 (0.28)
8		3.64 (0.36)	4.07 (0.35)	3.23 (0.48)	3.84 (0.47)	4.31 (0.26)	3.73 (0.31)	4.07 (0.30)
9		3.81 (0.37)	4.26 (0.36)	3.31 (0.51)	3.97 (0.50)	4.20 (0.27)	3.77 (0.33)	4.14 (0.32)
10		3.82 (0.37)	4.25 (0.36)	3.62 (0.56)	4.33 (0.54)	4.16 (0.25)	3.87 (0.35)	4.25 (0.34)
11		4.14 (0.42)	4.68 (0.42)	4.47 (0.64)	5.26 (0.63)		4.30 (0.46)	4.97 (0.45)
12		4.44 (0.50)	5.04 (0.50)	4.13 (0.68)	5.03 (0.68)		4.29 (0.50)	5.03 (0.50)
13		3.53 (0.49)	4.03 (0.49)	4.01 (0.66)	4.79 (0.66)		3.77 (0.48)	4.41 (0.48)
14		4.25 (0.47)	4.92 (0.47)	3.89 (0.68)	4.77 (0.68)	4.21 (0.25)	4.12 (0.44)	4.63 (0.44)
15	3.83 (0.17)	3.34 (0.51)	4.01 (0.51)	3.56 (0.71)	4.49 (0.71)		3.58 (0.49)	4.11 (0.49)
16	4.05 (0.14)	3.76 (0.53)	4.38 (0.52)	4.38 (0.73)	5.34 (0.73)		4.07 (0.52)	4.59 (0.51)
17	4.06 (0.18)	4.16 (0.54)	4.86 (0.53)	3.91 (0.62)	4.78 (0.62)		4.05 (0.45)	4.57 (0.44)
18	4.95 (0.11)	3.67 (0.35)	4.48 (0.34)				4.31 (0.25)	4.72 (0.24)
19	4.45 (0.14)						4.45 (0.14)	4.45 (0.14)

[a]From results for $Fe_n^+ + N_2 \rightarrow Fe_nN^+ + N$.
[b]From results for $Fe_n^+ + N_2 \rightarrow Fe_{n-1}N^+ + Fe + N$.
[c]From results for $Fe_n^+ + N_2 \rightarrow Fe_{n-2}N^+ + 2Fe + N$.
[d]Reference 46, average results for $Fe_m^+ + ND_3 \rightarrow Fe_mN^+ + D_2 + D$ and $Fe_m^+ + ND_3 \rightarrow Fe_{m-1}N^+ + Fe + D_2 + D$. Tight transition state.
[e]Average values of all results listed.
[f]Average values of all results except the direct bond energies.

same values of the parameter N in Eq. (4), i.e., those in Table III. The threshold obtained from this procedure differs from that used to synthesize the Fe_nN^+ cross section [that from Eq. (8)] by the competitive shift. This shift is added to the average STS bond energies in Table IV to yield a revised estimate for $D_0(Fe_n^+–N)$ and, using Eq. (8), the true threshold, $E_0(Fe_nN_2^+)$. This revised threshold is then used to recalculate a cross section for Fe_nN^+ in competition with $Fe_{n-1}N_2^+$. The process is repeated until the values of $D_0(Fe_n^+–N)$ and $E_0(Fe_nN^+)$ converge, which takes about three iterations. The revised thresholds, competitive shifts, and revised bond energies of the cluster nitrides are listed in Table V and shown in Fig. 9. We find that the competitive shifts range between 0.1 and 1.1 eV for clusters n=4–19. For reasons discussed below, these are believed to be the most reliable values for $D_0(Fe_n^+–N)$.

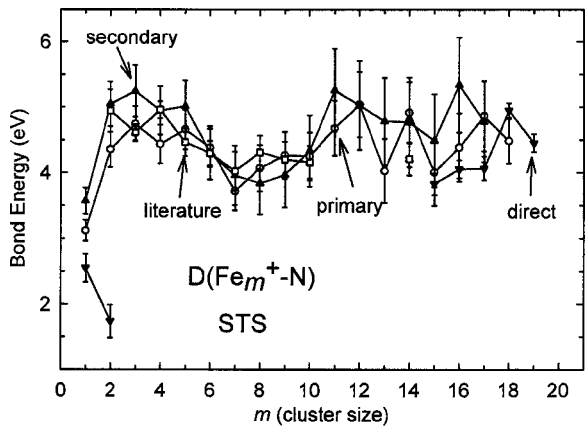

FIG. 8. Comparison of the 0 K cluster nitride bond energies obtained from direct (closed inverted triangles), primary (open circles), and secondary (closed triangles) measurements listed in Table IV as a function of the number of iron atoms m. Open squares indicate the 0 K values obtained from previous work on reactions with ND_3 (Ref. 46).

TABLE V. Summary of revised thresholds and 0 K bond energies (in eV) for Fe_m^+–N. (Uncertainties of one standard deviation in parentheses).

m	$E_0(Fe_m^+–N)$[a]	Competitive shifts	$D_0(Fe_m^+–N)$[b]
4	4.30 (0.26)	0.68	5.46 (0.26)
5	3.98 (0.26)	1.07	5.78 (0.26)
6	4.64 (0.26)	0.79	5.12 (0.26)
7	4.88 (0.28)	0.98	4.88 (0.28)
8	4.86 (0.30)	0.83	4.90 (0.30)
9	4.71 (0.32)	0.91	5.05 (0.32)
10	4.57 (0.34)	0.94	5.19 (0.34)
11	4.28 (0.45)	0.51	5.48 (0.45)
12	4.21 (0.50)	0.52	5.55 (0.50)
13	4.97 (0.48)	0.38	4.79 (0.48)
14	4.15 (0.44)	0.98	5.61 (0.44)
15	5.03 (0.49)	0.63	4.73 (0.49)
16	4.58 (0.51)	0.59	5.18 (0.51)
17	5.09 (0.44)	0.10	4.67 (0.44)
18	4.67 (0.24)	0.37	5.09 (0.24)
19	5.16 (0.14)	0.15	4.60 (0.14)

[a]Average threshold values of the STS model revised with competitive shifts.
[b]Bond energies including the effects of competitive shifts.

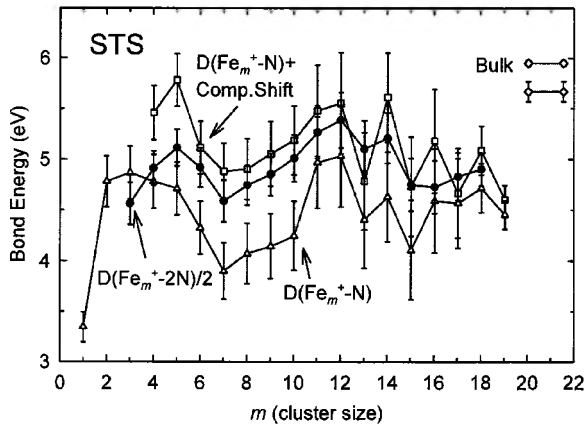

FIG. 9. Comparison of the average cluster dinitride bond energies, $D_0(Fe_m^+-2N)/2$, obtained from Table II (closed circles) with the average cluster nitride bond energies, $D_0(Fe_m^+-N)$, with (open squares, from Table V) and without (open triangles, from Table IV) corrections for competitive shifts. The range in estimated bulk-phase values for N binding to iron surfaces is shown to the right. The upper value comes from the estimates of Boszo *et al.* (Refs. 5 and 6) and the lower value comes from Stoltze and Nørskov's (Ref. 8) calculation (see text).

It might be imagined that both cluster dinitride and cluster nitride products also compete with the CID process, which could raise the bond energies measured above even further. However, CID is generally considered to involve a collision between Fe_n^+ and N_2 that need not yield a long-lived $Fe_nN_2^+$ intermediate whereas N_2 activation clearly requires such an intermediate. Thus we believe that reactions (2) and (3) do not compete directly with reaction (1) and therefore have not included this competition in our modeling.

DISCUSSION

Reaction mechanism

The mechanism for the reaction of iron cluster ions with N_2 appears fairly straightforward. The dominant products over the whole energy range observed are the cluster fragments, which result primarily from direct CID for all clusters, i.e., collisions in which the N_2 reactant provides a means to convert translational to internal energy of the cluster but fails to interact chemically with the cluster. Presumably, a weakly bound $Fe_n^+(N_2)$ physisorbed complex can be formed in some collisions, and can lead to N_2 activation and the formation of a cluster dinitride, $Fe_nN_2^+$. Our results for larger clusters indicate that this is an activated process involving a barrier of about 0.5 eV. Because the adsorption energy for molecular nitrogen is weak (less than about 0.4 eV on iron surfaces[76] and 0.56 ± 0.06 eV on atomic Fe^+),[77] the physisorbed complex is short lived and N_2 activation is a relatively rare event. However, once the cluster dinitrides are formed, the $Fe_nN_2^+$ clusters dissociate primarily by iron atom loss to form smaller cluster dinitride ions because iron-nitrogen bonds are stronger than iron-iron bonds. In competition with this, loss of N atoms can also occur at higher collision energies. As the kinetic energy of the reactant is increased, the primary products dissociate further with loss of atomic iron again being the most prominent dissociation process for both cluster dinitrides and nitrides. Our previous study demonstrated that small iron cluster ions, $Fe_n^+(n=2-19)$ dissociate via evaporation, i.e., sequential loss of iron atoms,[39] and a similar result is found here. No evidence for a molecularly bound FeN product fragment is found. This is demonstrated quantitatively by the agreement between the primary (or secondary) and direct measurements of the cluster nitride bond energies, because loss of FeN should have a threshold lower than loss of Fe and N by about 3.56 eV, the FeN bond energy calculated by Chertihin *et al.*[78] For the higher order dissociation pathways, the evaporation process is demonstrated by the sequential order in which the fragment ions are formed, and the observation that the energy spacings between neighboring product ions are typically 2–3 eV, comparable with the bare iron cluster ion bond energies.[39]

Comparison between the cluster nitride and dinitride bond energies

The various iron cluster-nitrogen bond energies derived above using the STS model are shown as a function of cluster size in Fig. 9. The LTS model yields similar patterns but smaller BDEs for the larger clusters. It can be seen that the lower Fe_m^+-N bond energies shown come from thresholds for formation of Fe_mN^+ shifted to higher energies by competition with the cluster dinitrides products. The upper Fe_m^+-N bond energies include the correction for this competition, estimated as outlined above. It can be seen that the latter values, which range between about 4.6 and 5.8 eV, agree fairly well with half the Fe_m^+-2N bond energies (except for $m=4$ and 5), having a range of about 4.5–5.5 eV, and are well within the combined experimental errors. If the latter set of Fe_m^+-N bond energies is more accurate, this suggests that the first and second nitrogen atoms bind similarly to iron cluster cations, comparable to results for the bond energies of the first and second oxygen atoms bound to iron cluster cations.[28] If the former set of Fe_m^+-N bond energies were accurate, the second nitrogen atom would be found to bind more strongly than the first nitrogen atom by up to 1.6 eV, a result that would be difficult to rationalize. Conservatively, the two sets of Fe_m^+-N bond energies can be considered as lower and upper limits to the true values, however, it seems likely that the values that include the competitive shift are probably more accurate.

It can be seen that the bond energies for Fe_m^+-xN ($m=7$, 13, 15, and 19, $x=1$ and 2) are relatively low compared to the values for their neighboring clusters. In previous work, the relative stability of different-sized transition metal clusters has been examined.[24] In general, it is found that these clusters favor compact geometries that are especially stable when they reach highly symmetric structures. For iron cation clusters, the Fe_n^+ clusters where $n=7$, 13, 15, and 19 are particularly stable. Thus, the weaker nitride bonds reflect the higher disruption energy needed to form the cluster nitride bonds for these clusters.

Another potentially significant result is the large difference (about 0.6 eV) observed in $D_0(Fe_m^+-N)$ vs $D_0(Fe_m^+-2N)/2$ for clusters $m=4$ and 5. This result may be related to the findings of Mortensen *et al.*, who calculated

that nitrogen atoms bind most strongly to iron surfaces in fourfold sites, e.g., on Fe(100), whereas binding to the (111) and (110) surfaces is weaker by 0.7 eV.[79] As small clusters will generally have threefold but no fourfold sites, it is possible that these clusters need to rearrange to accommodate formation of a strong nitride bond. Because Fe_m^+–N bond energies exceed Fe_m^+–Fe bond energies, dissociative chemisorption of N_2 should provide enough energy for such rearrangements. Clearly, the smallest clusters may not be able to accommodate formation of two strong nitride bonds, whereas larger clusters can disperse the two ligands to more separate sites. Such behavior may also explain why $D_0(Fe_m^+–N) < D_0(Fe_m^+–2N)/2$ for the stable $m=13$ atom cluster. Here, the energy necessary to disrupt this stable cluster in order to form a strong nitride bond is paid by the first ligand, such that the second nitride bond energy is apparently stronger.

Comparison to bulk phase thermochemistry

In previous studies, we have found a correspondence between the bond energies of D and O atoms to medium sized metal clusters ions ($n \approx 10–20$) of V, Cr, Fe, Co, and Ni.[27–33,46,47,80–84] As noted in the introduction, thermochemistry of N bound to iron surfaces is available but the interpretation is not unambiguous. For nitrogen based species, the binding of N atoms to Fe(100), Fe(110), and Fe(111) surfaces has been measured by Boszo *et al.*[5,6] who combined temperature-programmed desorption measurements of N_2 on these surfaces (2.52, 2.47, and 2.25 eV, respectively, at temperatures near 900 K) with activation energies for N_2 adsorption (0.22, 0.30, and 0.00 eV, respectively, measured near 700 K). This yields binding energies for N atoms to these iron surfaces of 6.05±0.03 eV at about 800 K of 5.95±0.03 eV, when converted to 0 K. However, Benziger has estimated that dissociative chemisorption of N_2 on iron surfaces should have an activation barrier of about 0.4±0.05 eV,[48] which exceeds the measurements of Boszo *et al.*[5,6] This estimate agrees nicely with the 0 K activation barrier we measure here of 0.48±0.03 eV. Thus our results indicate that the desorption bond energies should probably be reduced by another 0.1–0.2 eV, or $D_0(Fe(s)–N) = 5.8±0.1$ eV. We also note that these bulk-phase measurements for $D(Fe(s)–N)$ use Redhead's formula[5,6,85] and assume first-order desorption kinetics with a "normal" frequency factor of 10^{13} s^{-1}. A crucial factor for using Redhead's method is the availability of reliable preexponential factors,[86] which are commonly assumed to be on the order of $10^{13}–10^{15}$ s^{-1}. However, the assumption of constant preexponential factors can be problematic[86] and could result in additional errors in these measurements. Indeed, Stoltze's and Nørskov's work,[8] which takes into account the very low sticking coefficient for N_2 on iron surfaces, used a preexponential factor of $\sim 10^7$ s^{-1}.[4] (This assumes microscopic reversibility, which may not necessarily hold partly because of the various precursor states for N_2 adsorbed to iron surfaces.) Nevertheless, this lowered preexponential factor leads to a bulk phase value for $D(Fe(s)–N)$ of 5.76 eV (over a temperature range of 650–775 K), which we convert to an approximate 0 K value of 5.67 eV, in reasonable agreement with the 5.8±0.1 eV value noted above. Using this value, one of the most influential input factors, they obtained excellent agreement between their computed rates for ammonia synthesis and experimentally measured rates.[8] Alternatively, the adsorption bond energies to surfaces have been estimated from bulk compounds. In the case of Fe_4N, this leads to an estimate for binding of N atoms to iron surfaces of 5.0 eV,[48] well below the values from thermal desorption.

The 0 K Fe_m^+–N bond energies for clusters ($m=4–19$) measured by assuming an STS and corrected for the competitive shift (Table V) have an average of 5.1±0.4 eV, with the largest values ($m=4$, 5, 11, 12, 14) averaging to 5.6±0.3 eV. Likewise, the largest of the $D_0(Fe_m^+–2N)/2$ values are only slightly lower, 5.3±0.2 eV. These values compare nicely to the lower limit on the bulk phase thermal desorption values, 5.8±0.1 eV, which correspond to values corrected for a barrier of about 0.5 eV, as found in the present studies, as well as the 5.7 eV value suggested by Stoltze and Nørskov.[8] However, $D_0(Fe_m^+–N)$ values for the largest clusters ($m=15–19$) are 5.0±0.2 eV, suggesting that these larger clusters may not be representative of bulk-phase binding for reasons that are unclear. This behavior is in contrast to our measurements of bond energies for Fe_m^+–D,[27] Fe_m^+–O,[28] Fe_m^+–C, Fe_m^+–CD, and Fe_m^+–CD_2 (Ref. 47) which all reach a nearly constant value for larger clusters ($m \approx 10–20$). In cases where bulk phase values exist (D and O), the bulk phase thermochemistry agrees nicely with the asymptotic cluster bond energies. This difference in behavior cannot be attributed to the bond strengths of the products as the iron cluster bonds to O and N are comparable and greatly exceed those for D. What differs in these systems is the strength of the initial bond, $D_0(N_2)=9.76$ eV $\gg D_0(O_2)=5.12$ eV $> D_0(D_2)=4.55$ eV, which in turn determines whether the bond activation process is activated (requires passing over a tight transition state in the entrance channel). As discussed above, because of the very strong N_2 bond, cleavage of this molecule is clearly an activated process whereas D_2, O_2, and CD_4 activation generally is not. An unactivated process means that the energy released upon dissociative chemisorption is fully available to the transient $Fe_nX_2^+$ intermediate. This energy should help the intermediate self-anneal, allowing the intermediate to find the most stable structure of the resulting products, $Fe_{n-1}X_2^+$ and Fe_nX^+. In contrast, the activated process means that only a small fraction of the initial reactants can lead to the $Fe_nX_2^+$ intermediate, which makes the reaction much more sensitive to the details of the electronic and geometric structure of the reactant cluster. Depending on the cluster size, the subsequent dynamics of the reaction may be altered and the extent of the self-annealing process restricted. As a consequence, the cluster nitride and dinitride bond energies do not reach the bulk phase limit although it appears that several clusters approach this value.

The various iron nitride bond energies can also be compared to previous measurements in our laboratory of the isoelectronic Fe_m^+–CD species.[47] These have an average bond energy of 5.0±0.2 eV for $m=3–10$ and of 5.9±0.4 eV for larger clusters ($m=11–15$). For the smaller clusters

($m=3-12$), these Fe_m^+-CD bond energies lie within experimental error of the $D_0(Fe_m^+-2N)/2$ and $D_0(Fe_m^+-N)$ values obtained with the competitive shift, again suggesting that the latter values are our most reliable. For larger clusters, ($m=13-15$), the Fe_m^+-CD bond energies are greater than those for Fe_m^+-N (with the competitive shift) by $0.7-1.2\pm0.4$ eV. In general, the Fe_m^+-CD and Fe_m^+-N bond energies are comparable to one another, consistent with the isoelectronic CD and N adsorbates both forming strong bonds characteristic of a triple bond to the cluster.[47]

The energy of adsorption of the N atom on iron surfaces is a critical value in understanding dissociative adsorption of nitrogen, the rate-limiting step in the Haber process for ammonia synthesis. The present results appear to confirm that the estimates of Ertl and coworkers for this adsorption energy are too high, whereas the revised values suggested by Benziger[48] and Stoltze and Nørskov[8] are reasonable.

ACKNOWLEDGMENT

This research is supported by the Chemical Sciences, Geosciences, and Biosciences Division, Office of Basic Energy Sciences, U. S. Department of Energy.

[1] D. M. Samuel, *Industrial Chemistry-Inorganic* (Royal Society of London, London, 1970).
[2] *A Treatise on Dinitrogen Fixation*, edited by R. W. F. Hardy and F. R. C. Bottomley (Wiley-Interscience, New York, 1979).
[3] H. Conrad, G. Ertl, J. Küppers, and E. E. Latta, Surf. Sci. **57**, 475 (1976).
[4] R. Raval, M. A. Harrison, and D. A. King, in *The Chemical Physics of Solid Surfaces and Heterogeneous Catalysis*, edited by D. A. King and D. P. Woodruff (Elsevier, New York, 1990), Vol. 3A, pp. 75–92.
[5] F. Boszo, G. Ertl, M. Grunze, and M. Weiss, J. Catal. **49**, 18 (1977).
[6] F. Boszo, G. Ertl, and M. Weiss, J. Catal. **50**, 519 (1977).
[7] G. Ertl, S. B. Lee, and M. Weiss, Surf. Sci. **114**, 515 (1982).
[8] P. Stoltze and J. Nørskov, Phys. Rev. Lett. **55**, 2502 (1985).
[9] M. Grunze, M. Golze, W. Hirschwald, H. J. Freund, H. Pulm, U. Seip, M. C. Tsai, G. Ertl, and J. Küppers, Phys. Rev. Lett. **53**, 850 (1984).
[10] S. T. Rettner, H. E. Pfnür, H. Stein, and D. J. Auerbach, J. Vac. Sci. Technol. A **6**, 899 (1988).
[11] S. Westerberg, C. Wang, K. Chou, and G. A. Somorjai, J. Phys. Chem. B **108**, 6374 (2004).
[12] M. Ø. Pedersen, L. Österlund, J. J. Mortensen, M. Mavrikakis, L. B. Hansen, I. Stensgaard, E. Lægsgaard, J. K. Nørskov, and F. Besenbacher, Phys. Rev. Lett. **84**, 4898 (2000).
[13] M. D. Morse, Chem. Rev. (Washington, D.C.) **86**, 1049 (1986).
[14] M. M. Kappes, Chem. Rev. (Washington, D.C.) **88**, 372 (1988).
[15] D. C. Parent and S. L. Anderson, Chem. Rev. (Washington, D.C.) **92**, 1541 (1992).
[16] P. B. Armentrout, J. B. Griffin, and J. Conceição, in *Progress in Physics of Clusters*, edited by G. N. Chuev, V. D. Lakhno, and A. P. Nefedov (World Scientific, Singapore, 1999), p. 198.
[17] P. B. Armentrout, Annu. Rev. Phys. Chem. **52**, 423 (2001).
[18] J. Conceição, R. T. Laaksonen, L.-S. Wang, T. Guo, P. Nordlander, and R. E. Smalley, Phys. Rev. B **51**, 4668 (1995).
[19] P. Fayet, M. J. McGlinchey, and L. H. Wöste, J. Am. Chem. Soc. **109**, 1733 (1987).
[20] S. Vajda, S. Wolf, T. Leisner, U. Busolt, and L. H. Wöste, J. Chem. Phys. **107**, 3492 (1997).
[21] M. Ichihashi, T. Hanmura, R. T. Yadav, and T. Kondow, J. Phys. Chem. A **104**, 11885 (2000).
[22] K. P. Kerns, E. K. Parks, and S. J. Riley, J. Chem. Phys. **112**, 3394 (2000).
[23] P. A. Hintz and K. M. Ervin, J. Chem. Phys. **100**, 5715 (1994).
[24] P. B. Armentrout, D. A. Hales, and L. Lian, in *Advances in Metal and Semiconductor Clusters*, edited by M. A. Duncan (JAI, Greenwich, 1994), Vol. 2, pp. 1–39.
[25] P. B. Armentrout and B. L. Kickel, in *Organometallic Ion Chemistry*, edited by B. S. Freiser (Kluwer, Dordrecht, 1996), pp. 1–45.
[26] P. B. Armentrout, Int. J. Mass. Spectrom. **200**, 219 (2000).
[27] J. Conceição, S. K. Loh, L. Lian, and P. B. Armentrout, J. Chem. Phys. **104**, 3976 (1996).
[28] J. B. Griffin and P. B. Armentrout, J. Chem. Phys. **106**, 4448 (1997).
[29] J. B. Griffin and P. B. Armentrout, J. Chem. Phys. **107**, 5345 (1997).
[30] J. B. Griffin and P. B. Armentrout, J. Chem. Phys. **108**, 8062 (1998).
[31] J. B. Griffin and P. B. Armentrout, J. Chem. Phys. **108**, 8075 (1998).
[32] J. Xu, M. T. Rodgers, J. B. Griffin, and P. B. Armentrout, J. Chem. Phys. **108**, 9339 (1998).
[33] J. Conceição, R. Liyanage, and P. B. Armentrout, Chem. Phys. **262**, 115 (2000).
[34] V. A. Spasov, H. T. Lee, and K. M. Ervin, J. Chem. Phys. **112**, 1713 (1995).
[35] Y. Shi, V. A. Spasov, and K. M. Ervin, J. Chem. Phys. **111**, 938 (1999).
[36] K. M. Ervin, Int. Rev. Phys. Chem. **20**, 127 (2001).
[37] H. T. Deng, K. P. Kerns, and A. W. Castleman, Jr., J. Phys. Chem. **100**, 13386 (1996).
[38] R. C. Bell, K. A. Zemski, D. R. Justes, and A. W. Castleman, Jr., J. Phys. Chem. **114**, 798 (2001).
[39] L. Lian, C. X. Su, and P. B. Armentrout, J. Phys. Chem. **97**, 4072 (1992).
[40] C. X. Su, D. A. Hales, and P. B. Armentrout, J. Chem. Phys. **99**, 6613 (1993).
[41] C. X. Su, D. A. Hales, and P. B. Armentrout, Chem. Phys. Lett. **201**, 199 (1993).
[42] C. X. Su and P. B. Armentrout, J. Chem. Phys. **99**, 6506 (1993).
[43] D. A. Hales, C. X. Su, and P. B. Armentrout, J. Chem. Phys. **100**, 1049 (1994).
[44] L. Lian, C. X. Su, and P. B. Armentrout, J. Chem. Phys. **96**, 7542 (1992).
[45] D. A. Hales, L. Lian, and P. B. Armentrout, Int. J. Mass Spectrom. Ion Process. **102**, 269 (1990).
[46] R. Liyanage, J. B. Griffin, and P. B. Armentrout, J. Chem. Phys. **119**, 8979 (2003).
[47] R. Liyanage, X. G. Zhang, and P. B. Armentrout, J. Chem. Phys. **115**, 9747 (2001).
[48] J. B. Benziger, in *Metal-Surface Reaction Energetics*, edited by E. Shustorovich (VCH, New York, 1991), pp. 53–107.
[49] J. D. Cox, D. D. Wagman, and V. A. Medvedev, *CODATA Key Values for Thermodynamics* (Hemisphere, New York, 1989).
[50] S. K. Loh, D. A. Hales, L. Lian, and P. B. Armentrout, J. Chem. Phys. **90**, 5466 (1989).
[51] D. Gerlich, Adv. Chem. Phys. **82**, 1 (1992).
[52] N. R. Daly, Rev. Sci. Instrum. **31**, 264 (1960).
[53] K. M. Ervin and P. B. Armentrout, J. Chem. Phys. **83**, 166 (1985).
[54] J. D. Burley, K. M. Ervin, and P. B. Armentrout, Int. J. Mass Spectrom. Ion Process. **80**, 153 (1987).
[55] P. B. Armentrout, J. Am. Soc. Mass Spectrom. **13**, 419 (2002).
[56] S. K. Loh, E. R. Fisher, L. Lian, R. H. Schultz, and P. B. Armentrout, J. Phys. Chem. **93**, 3159 (1989).
[57] See EPAPS Document No. E-JCPSA6-124-013608 for 13 figures. This document can be reached via a direct link in the online article's HTML reference section or via the EPAPS homepage (http://www.aip.org/pubservs/epaps.html).
[58] M. T. Rodgers, K. M. Ervin, and P. B. Armentrout, J. Chem. Phys. **106**, 4499 (1997).
[59] R. H. Schultz, K. C. Crellin, and P. B. Armentrout, J. Am. Chem. Soc. **113**, 8590 (1991).
[60] F. A. Khan, D. E. Clemmer, R. H. Schultz, and P. B. Armentrout, J. Phys. Chem. **97**, 7978 (1993).
[61] T. Beyer and D. F. Swinehart, Comm. Assoc. Comput. Mach. **16**, 379 (1973).
[62] S. E. Stein and B. S. Rabinovitch, J. Chem. Phys. **58**, 2438 (1973); Chem. Phys. Lett. **49**, 183 (1977).
[63] R. G. Gilbert and S. C. Smith, *Theory of Unimolecular and Recombination Reactions* (Blackwell Science, Oxford, 1990).
[64] A. A. Shvartsburg, K. M. Ervin, and J. H. Frederick, J. Chem. Phys. **104**, 8458 (1996).
[65] N. F. Dalleska, K. Honma, and P. B. Armentrout, J. Am. Chem. Soc. **115**, 12125 (1993).
[66] J. L. Elkind and P. B. Armentrout, J. Am. Chem. Soc. **90**, 6576 (1986).
[67] P. B. Armentrout, Int. Rev. Phys. Chem. **9**, 115 (1990).
[68] P. B. Armentrout, in *Advances in Gas Phase Ion Chemistry*, edited by N. G. Adams and L. M. Babcock (JAI, Greenwich, 1992), Vol. 1, p. 83.
[69] D. E. Clemmer, Y.-M. Chen, N. Aristov, and P. B. Armentrout, J. Chem. Phys. **98**, 7538 (1994).

[70] D. G. Truhlar, B. C. Garrett, and S. J. Klippenstein, J. Phys. Chem. **100**, 12771 (1996).
[71] K. A. Holbrook, M. J. Pilling, and S. H. Robertson, *Unimolecular Reactions*, 2nd ed. (Wiley, New York, 1996).
[72] W. Kauffman, R. H. Hauge, and J. L. Margrave, High. Temp. Sci. **17**, 237 (1984).
[73] F. Muntean and P. B. Armentrout, J. Phys. Chem. B **106**, 8117 (2002).
[74] M. F. Jarrold and J. E. Bower, J. Chem. Phys. **87**, 5728 (1987).
[75] M. T. Rodgers and P. B. Armentrout, J. Chem. Phys. **109**, 1787 (1998).
[76] G. Ertl, Catal. Rev.-Sci. Eng. **21**, 201 (1980).
[77] B. L. Tjelta and P. B. Armentrout, J. Phys. Chem. A **101**, 2064 (1997).
[78] G. V. Chertihin, L. Andrews, and M. Neurock, J. Phys. Chem. **100**, 14609 (1996).
[79] J. J. Mortensen, M. V. Ganduglia-Pirovano, L. B. Hansen, B. Hammer, P. Stoltze, and J. K. Nørskov, Surf. Sci. **422**, 8 (1999).
[80] F. Liu, F.-X. Li, and P. B. Armentrout, J. Chem. Phys. **123**, 064304/1 (2005).
[81] F. Liu and P. B. Armentrout, J. Chem. Phys. **122**, 194320/1 (2005).
[82] D. Vardhan, R. Liyanage, and P. B. Armentrout, J. Chem. Phys. **119**, 4166 (2003).
[83] F. Liu, R. Liyanage, and P. B. Armentrout, J. Chem. Phys. **117**, 132 (2002).
[84] R. Liyanage, J. Conceição, and P. B. Armentrout, J. Chem. Phys. **116**, 936 (2002).
[85] P. A. Redhead, Vacuum **12**, 203 (1962).
[86] K. R. Parseba and A. J. Gellmann, Phys. Rev. Lett. **86**, 4338 (2001).